Assessing the effects of earlier snow melt-out on Alpine shrub growth: the sooner the better?

L. Francon, Thierry Ameglio, Christophe Corona, I. Till-Bottraud, P. Choler, B.Z. Carlson, Guillaume Charrier, S. Morin, Nicolas Eckert, E. Roussel, et al.

Assessing the effects of earlier snow melt-out on Alpine shrub growth: the sooner the better?

L. Francon[1*], C. Corona[1], I. Till-Bottraud[1], P. Choler[2], B. Carlson[3], G. Charrier[4,5], T. Améglio[4,5], S. Morin[6], N. Eckert[7], E. Roussel[1], J. Lopez-Saez[8], M. Stoffel[8,9,10]

[1]Université Clermont Auvergne, CNRS, Geolab, F-63000 Clermont-Ferrand, France
[2] Université Grenoble Alpes, Université Savoie Mont-Blanc, CNRS, LECA, F-38000 Grenoble, France
[3] Centre de Recherches sur les Ecosystèmes d'Altitude (CREA), Observatoire du Mont-Blanc, 74400 Chamonix, France
[4] Université Clermont Auvergne, F-63000 Clermont-Ferrand, France
[5] INRA, PIAF, F-63000 Clermont-Ferrand, France
[6] Météo-France – CNRS, CNRM UMR 3589, Centre d'Études de la Neige, Grenoble, France
[7] Université Grenoble Alpes, Irstea, UR ETGR, F-38000 Grenoble, France
[8] Climate Change Impacts and Risks in the Anthropocene (C-CIA), Institute for Environmental Sciences, University of Geneva, Geneva, Switzerland.
[9] Department of Earth Sciences, University of Geneva, Geneva, Switzerland.
[10] Department F.-A. Forel for Environmental and Aquatic Sciences, University of Geneva, Geneva, Switzerland.
*Contact information: loic.francon@etu.uca.fr

Abstract

Enhanced shrub growth in a warming alpine climate has potential far-reaching implications, including soil nutrient cycling, carbon storage, or water and surface energy exchanges. Growth ring analysis can yield mid- to long-term, annually resolved records of shrub growth, and thereby offer valuable insights into how growth is driven by interannual climate variability. In the European Alps, dendroecological approaches have shown that dwarf shrub productivity is influenced by interannual variations of growing season temperature but results also point to a negative effect of winter precipitation on radial growth. However, as past work lacked snow cover data, links between snow cover duration, growing season length, energy availability and inter-annual shrub growth remain poorly understood.

In this paper, we combined multi-decadal shrub-ring series from 49 individuals sampled at three sites along a 600-m elevational gradient in the Taillefer massif, located in the French Alps to assess growth sensitivity of long-lived and widespread *Rhododendron ferrugineum* shrubs to both snow cover dynamics and temperature changes. To this end, we computed structural equation models to track the response of shrub radial growth to extending growing season at 1800, 2000 and 2400 m above sea level and for two time periods (i.e. 1959-1988 and 1989-2016). The second period is marked by a significant advance in snow melt-out resulting in a regime shift highlighted at the end of the 1980s by a breakpoint analysis.

At the high-elevation site, our results demonstrate a positive effect of increasing growing season length on shrub growth, which is strongly dependent on snowpack depth and snow cover duration. Conversely, at lower elevations, earlier melt-out dates and associated late frost exposure are shown to lead to radial growth reduction. Moreover, the climate signal in ring-width chronologies of *R. ferrugineum* portrays a weakening since 1988 – similar to a phenomenon observed in series from circumpolar and alpine tree-ring sites and referred to as "divergence".

By analyzing long-term records of radial growth along an elevation gradient, our work provides novel insights into the complex responses of shrub growth to climate change in alpine environments. This paper demonstrates that *R. ferrugineum*, as a dominant alpine shrub species, behave as an ecological indicator of the response of alpine ecosystem to global warming.

Keywords

dendrochronology; dendroecology; shrub expansion; dwarf shrubs; *Rhododendron ferrugineum*; Structural Equation Model; divergence; elevation gradient; frost; snow cover

Introduction

Temperatures in Arctic and Alpine regions have been increasing twice as fast as the global average over the last decades (Stocker et al., 2013), with potential far-reaching consequences for ecosystem functioning due to feedbacks between vegetation and climate (Bjorkman et al., 2018, 2020; Pearson et al., 2013). Rapid climate warming is also driving changes in the structure and composition of cold ecosystems and has been associated with changes in plant phenology, diversity and richness (Boscutti et al., 2018; Grabherr et al., 1994; Myers-Smith et al., 2019; Steinbauer et al., 2018), poleward and upslope shifts in species geographic distribution (Chen et al., 2011; Elsen and Tingley, 2015; Lenoir et al., 2008; Parmesan and Yohe, 2003; Walther et al., 2002) and thermophilization (Dolezal et al., 2016; Elmendorf et al., 2015; Gottfried et al., 2012). At high-latitude sites, increasing vegetation productivity (Pearson et al., 2013) associated with a widespread shrub expansion (Elmendorf et al., 2015; Sturm et al., 2001; Tape et al., 2006) has resulted in a greening trend, characterized by increasing canopy cover, height, abundance, and biomass (Forbes et al., 2010; Hollesen et al., 2015; Myers-Smith et al., 2011, 2015a, 2020). Conversion of tundra to shrubland is driven by ongoing warming, and modulated by soil moisture (Ackerman et al., 2017; Elmendorf et al., 2012), but also by changes in snow cover duration (Gamm et al., 2018; Niittynen et al., 2018; Weijers et al., 2018a; Young et al., 2016). Recent warming and related shrubification (i.e. increasing shrub cover and biomass) in Arctic systems has also been shown to drive climate feedbacks, for instance by altering surface albedo, energy, water balance, or permafrost (Blok et al., 2011; Chapin, 2005; Liston et al., 2002; Sturm et al., 2001). Although comparable changes can be expected at high altitudes, shrubification has hitherto received very little consideration in temperate mountain systems.

In the European Alps, documentation of upslope advancement of shrub species remains scarce and spatially limited (Anthelme et al., 2007; Cannone et al., 2007; Dullinger et al., 2003; Malfasi and Cannone, 2020). At the regional scale, Carlson et al., (2017) provided remote sensing-based evidence linking the observed greening of alpine vegetation (increased productivity) to increasing air temperatures and decreasing snow cover duration. Snow manipulation experiments, designed to simulate the expected advance of melt-out dates in a warmer climate (Gerdol et al., 2013; Rixen et al., 2010; Wipf and Rixen, 2010) confirm the strong control of snowpack duration on shrub phenology and growth via indirect effects on soil temperature, nutrient availability and frost exposure. Despite the indisputable value of these studies to improve understanding of climate–growth linkages, experimental studies typically cover relatively short periods (1-2 years; Wipf and Rixen, 2010) and cannot capture longer-term shrub growth responses to climate change.

By contrast, growth-ring analyses have the potential to provide uninterrupted mid- to long-term, annually-resolved records of shrub growth, thereby revealing responses to interannual climate variability (Bär et al., 2006; Buchwal et al., 2013; Forbes et al., 2010; Hantemirov et al., 2000; Hollesen et al., 2015; Weijers et al., 2010; Young et al., 2016 and Myers-Smith et al., 2015b for an exhaustive review). Still underused in high-altitude environments, the limited number of existing dendroecological studies tends to confirm that dwarf shrub productivity is influenced by interannual variations of growing season temperature (Francon et al., 2017; Franklin, 2013; Liang et al., 2012; Liang and Eckstein, 2009; Lu et al., 2015; Pellizzari et al., 2014). In the Alps, initial results point to a negative effect of winter precipitation on the radial growth of shrubs (Carrer et al., 2019; Francon et al., 2017; Pellizzari et al., 2014; Rixen et al., 2010), a phenomenon that has been observed only rarely in circum-Arctic tundra ecosystems (Bär et al., 2008; Hallinger et al., 2010; Ropars et al., 2015; Zalatan and Gajewski, 2006; but see Schmidt et al., 2010, who found snow to correlate negatively with *Salix arctica* growth). Several hypotheses have been proposed to explain this phenomenon, such as the detrimental effect of late-persisting snow on the onset of cambial activity, growing season length or soil temperatures (Pellizzari et al., 2014). In the Alps, the positive effects of longer and warmer growing seasons could be offset by the negative effect of increased late-frost exposure due to earlier melt-out dates (Jonas et al., 2008; Rixen et al., 2012). Most of the previous dendroecological studies, however, relied on monthly-resolved meteorological time series and lacked snow cover data, thereby precluding a precise assessment of the relationships between snow cover duration, growing season length and energy availability during the snow free period. In addition, in the

Alps, existing dendroecological studies addressing the sensitivity of shrubs to climate have largely ignored the role of topography, and even more so changes along elevational gradients. We argue that by ignoring the impact of changes in snow cover alongside temperature at different elevations, shrub ring–climate studies focusing on plant growth in temperate mountain ecosystems will likely dismiss an obvious mechanistic pathway, which could potentially regulate shrub growth in response to winter snow accumulation. This knowledge gap is particularly pressing given the wealth of studies documenting a warming-induced decrease of snow cover duration in temperate alpine regions of North America (Mote et al., 2005) and Europe (Beniston et al., 2018; Hantel et al., 2000, 2012; López-Moreno, 2005). Ongoing and future climate change will likely accelerate warming, but also favor earlier melt-out dates and decreased snowpack depths at altitudes comprised between 1500 and 3000 m above sea level (asl; Beniston et al., 2018; Marty et al., 2017; Steger et al., 2013; Verfaillie et al., 2018).

Here, we investigate long-term relationships between snow cover dynamics and the growth of *Rhododendron ferrugineum* in the Taillefer massif where shrub growth is expected to be influenced by snow cover dynamics (Francon et al., 2017) and where plants are likely to be vulnerable to climate change. We use individuals sampled at three sites along a 600-m elevational gradient. In order to test the hypothesis that shrub growth is directly positively influenced by the accumulation of degree days received after the snow melt-out date (SFGDD), we (i) developed multidecadal shrub-ring series from long-lived *Rhododendron ferrugineum* individuals; (ii) evaluated recent climatic trends in atmospheric temperature, snow cover and SFGDD obtained from a locally calibrated meteorological model, specifically designed for the mountain environment and spanning the period 1958-2016 (Durand et al., 2009a, 2009b) and (iii) investigate climate–growth relationships using structural equation models (SEMs) designed to disentangle the effects of the above-mentioned climate variables on radial growth.

We computed SEMs for the periods 1959-1988 and 1989-2016 to test for the potential change in shrub sensitivity to climatic drivers in the context of recent climate changes.

Material and methods

Study species

Rhododendron ferrugineum L. is the dominant mountain shrub of the subalpine belt in the siliceous Alps (Ozenda, 1985). It is distributed from about 1600 to 2500 m asl, where it can form large heathlands or grow in localized patches (Escaravage et al., 1997). The high local abundance of the species can be attributed to complementary sexual and vegetative reproductive strategies (Doche et al., 2005) which enable *R. ferrugineum* to outcompete other plants (Pornon and Doche, 1996) and to reach a 90–100% cover after 150–250 years (Pornon and Doche, 1995). *R. ferrugineum* provides an ideal model to study the long-term effects of climate on radial growth due to its high longevity, estimated to be up to three centuries (Escaravage et al., 1998), as well as its clearly identifiable annual rings discriminated by a band of radially aligned, thick walled latewood fibers, flattened along the ring boundary (Francon et al., 2017).

Study area

The study area is situated in the northern French Alps (Fig. 1), on a northwest-facing slope in the Taillefer massif. At Taillefer, *R. ferrugineum* is the dominant species (80–100% cover) of above-treeline dwarf shrub heathlands. The species developed on abandoned pastures between 1900 and 2100 m asl and is intermixed with *Sorbus* sp. and *Vaccinium* sp. along with scattered *Picea abies* and *Pinus uncinata* trees. Beyond this altitude, heathlands become more fragmented and are mixed with patches of alpine meadows and scree. Isolated patches of *R. ferrugineum* are observed up to ~2500 m asl. Shrub individuals were sampled along an elevational gradient, at three sites located at (i) 1800-1850 m (SAL1800), (ii) 1950-2050 m (SAL2000) and (iii) 2300-2500 m asl (CN2400). SAL1800 and SAL2000 are located at the Côte des Salières (SAL, 45°02′N, 5°52′E, Fig. 1) on a northwest-facing slope with slope angles ranging from 23° to 33°. CN2400 is located in the Combe Nord (3 km east of SAL, 45°02′N, 5°55′E, Fig. 1) on a north-facing slope (25°). At SAL1800 and SAL2000, bedrock consists of amphibolite and gneissic gabbro (Doche et al., 2005). SAL1800 and SAL2000 heathlands have developed on stony, ochre-brown humic acidic soils (Pornon et al., 1997). At CN2400, *R. ferrugineum* individuals grow on shallow and discontinuous soils developed on talus slopes and weathered rock outcrops.

Climate of the Taillefer massif reflects a transition between the wet oceanic Pre-Alps (Chartreuse, Vercors) and the intra-alpine Oisans massif, with the latter being characterized by a more continental climate with drier summers (Pautou et al., 1992). Daily reanalysis from the SAFRAN meteorological system (Durand et al., 2009a) was used to characterize climatic conditions along the elevational gradient (Fig. 1B). Over the period 1959-2016, mean annual air temperatures were 4.2°C, 3.3°C, and 1.4°C at SAL1800, SAL2000 and CN2400, respectively. The melt-out date occurred on average on May 2 at 1800 m asl, and roughly one month later at 2400 m asl (June 6).

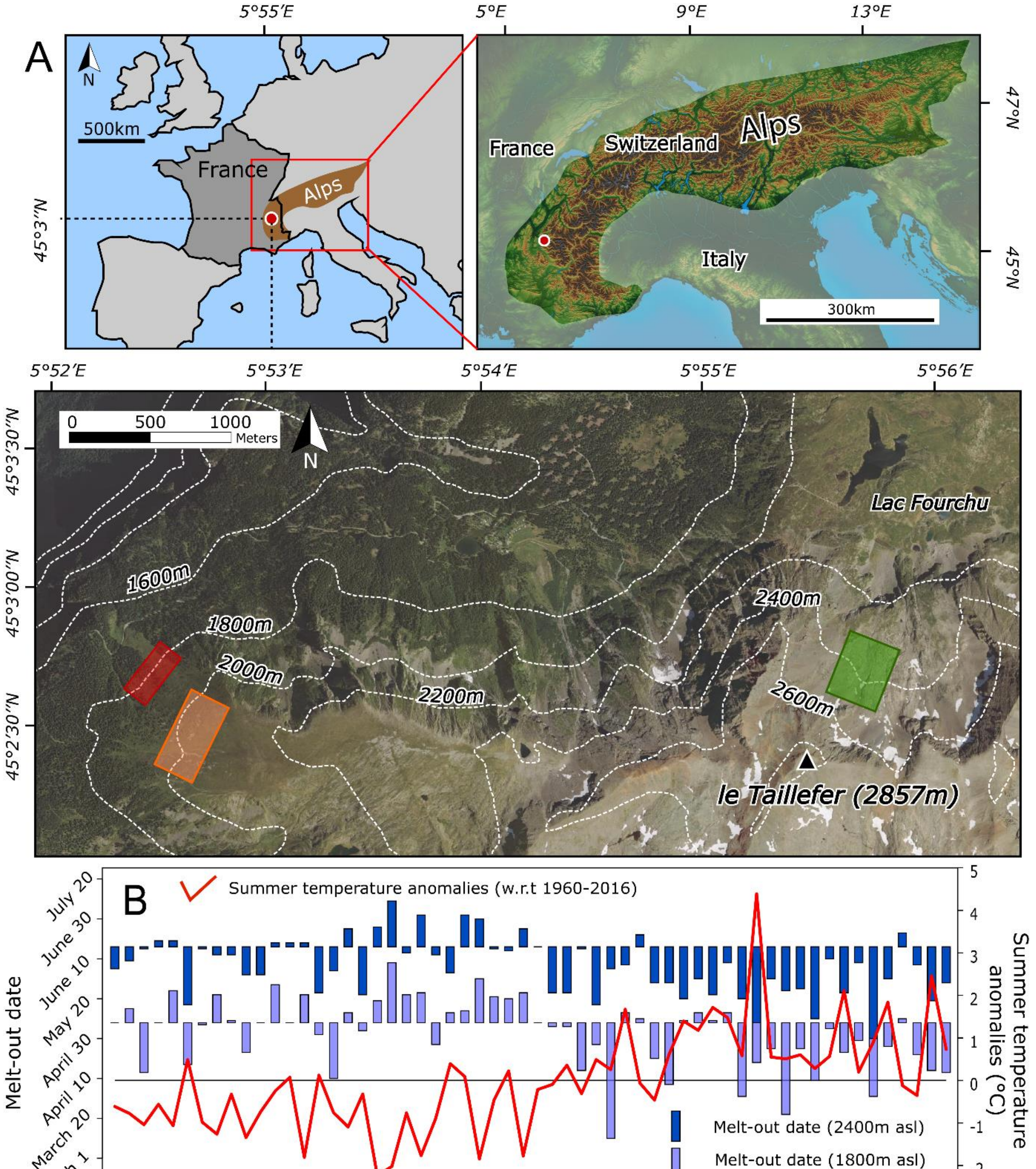

Figure 1: (A) Location of the study sites, Côte des Salières (SAL1800, red; SAL2000, orange) and Combe Nord (CN2400, green) in the Taillefer massif (French Alps). (B) Summer (May-August) temperature anomalies (1959-2016) as well as melt-out dates at 1800 (light blue) and 2400 m asl (dark blue) for the 1959-2017 period. Meteorological data were extracted from the SAFRAN-Crocus re-analysis datasets (Durand et al., 2009a, 2009b).

Sample collection and preparation

A total of 80 randomly selected *R. ferrugineum* individuals were sampled at the three sites: 36 at SAL2000 in October 2015, 17 at SAL1800, and 27 at CN2400 in October 2016. Individuals were sampled at a minimum distance of four meters from each other to avoid the sampling of the same clone (Escaravage et al., 1998). Locations were recorded with metric precision using a Trimble GeoExplorer GNSS (Global Navigation Satellite System) unit. Three to six wood sections were cut per individual on the main stems, starting at the root collar and then every 10-20 cm to the stem extremity. This approach was used in order to apply the serial-sectioning method, consisting of repeated growth-ring width measurements and cross dating at the intra-stem level (Kolishchuk, 1990).

To ensure precise detection of all rings, 20 µm thick cross sections were prepared from each sample using a slide microtome. Cross sections were then stained using Safranin and Astra Blue, and permanently fixed on microslides with Canada balsam (Schweingruber et al., 2011). High-resolution digital pictures were taken using a Carl Zeiss Axio Observer Z1 coupled to a Zeiss AxioCam MR R3 camera under 40–100 magnification. Individual images were merged automatically to cover the whole cross-sections by using the Zen 2011 software.

Crossdating and chronology development

Width of individual growth rings were measured from digital images with CooRecorder 7.6 (CYBIS Elektonik & Data AB) along three radii of the cross-sections to detect wedging rings. Radial measurements along the chosen radii were supplemented by careful visual inspection of each cross section to eliminate annual growth underestimation caused by partially missing rings. Cross-dating was based on a three-step procedure involving a comparison of growth curves (i) between three radii measured within a single cross section, (ii) among the mean growth curves of all sections within individual plants, and finally (iii) between the mean growth curves of all shrubs of a given site. The output of visual crossdating was statistically checked with COFECHA (Holmes, 1994).

After cross-dating, each individual mean series was standardized (Cook and Kairiukstis, 1990; Fritts, 1976) with a double-detrending process in ARSTAN (Cook, 1987). We first selected a negative exponential function to eliminate non-climatic trends (e.g. age-related growth trend and other potential biological effects) referred to as Neg-Exp chronologies. In addition, we fitted a cubic smoothing spline, preserving 50% of the variance at a wave-length of 32 years so as to remove the effect of localized disturbance events (Cook and Peters, 1981) hereafter referred to as detrended chronologies. In both approaches, outputs referred as growth indices were averaged by year using a bi-weighted robust mean aimed at reducing the influence of outliers and at developing mean standardized site chronologies (Cook and Peters, 1981). The resulting growth indices are referred to as ring-width indices (RWI).

Several descriptive statistics were then applied to detrended chronologies using the *dplR* package, including standard deviation (SD), first-order autocorrelation (AC), mean sensitivity (MS), mean inter-series correlation (Rbar), and expressed population signal (EPS; Bunn, 2008) in R 3.3.2 (R Core Team, 2016). Running Rbar and EPS were computed at each site using a 30-year moving window with a 29-year overlap to illustrate changes in the strength of common patterns of radial growth over time. We used the commonly applied quality threshold of EPS $\geq$ 0.85 to determine the reliability of our chronologies. As shrubs may potentially retain climate-driven, low frequency variations in the raw data (decadal growth variations), Neg-Exp chronologies were used to detect potential impacts of decadal-scale climatic fluctuations on radial growth. Indices from the double-detrending procedure were used for climate-growth correlations and climate-growth modeling in relation to high-frequency (interannual) growth variations.

Meteorological series

At each plot, daily meteorological and snow time series were obtained from the SAFRAN-Crocus coupled snowpack-atmosphere model. The SAFRAN reanalysis combines *in-situ* meteorological observations with synoptic-scale meteorological fields to provide continuous time series of meteorological variables at hourly resolution and for elevation bands of 300 m within areas, referred to as “massifs” (Oisans in the case of this study), assumed to be horizontally homogenous (Durand et al., 2009a). The dataset extends back to 1958. SAFRAN meteorological fields are used to drive a land surface model, the ISBA-Crocus soil and snowpack model. This tool provides corresponding reanalysis of snow conditions and underlying ground temperature for the same time span as SAFRAN reanalysis (Durand et al., 2009b; Vionnet et al., 2012). To quantify ground temperature, we extracted values for the uppermost soil layer with a thickness of 1 cm.

SAFRAN meteorological fields corresponding to the sampling sites were extracted according to their elevation, aspect, and slope angles (Lafaysse et al., 2013). Meteorological data were interpolated from the neighboring 300-m elevation bands, and incoming shortwave radiation data was adjusted by using the prevailing aspect and slope angle. The ISBA-Crocus models runs were performed specifically for the sites. Vegetation was represented in a simplified manner in the simulations, assuming grassy conditions so as to simulate typical snow conditions and underlying ground temperature for open areas, therefore neglecting small-scale interactions between vegetation, topography, and snowpack. We then extracted hourly air temperature and precipitation sums as well as daily snow depth and uppermost ground layer temperatures (6:00 UTC) for the period 1959-2017. The data were carefully visually checked to detect extreme temperature events that could be linked with marked growth reduction. Monthly minimum, mean, and maximum air temperature, monthly precipitation sums, snow depth, and duration, melt-out date, sum of snow-free growing degree days (SFGDD) and daily uppermost ground layer temperature series were computed from the same datasets. The snow melt-out date was defined as the last day when snow cover reached the mean height of the shrub canopy at *c*. 50 cm for SAL1800 and SAL2000, and at *c*. 30 cm for CN2400. SFGDD were calculated for periods with snow-free ground and daily air mean temperatures above zero degrees. SFGDD series were calculated from melt-out date to August 31.

Given that previous work identified a shift toward earlier snow melt-out in the study region occurring during the late 1980s (Dedieu et al., 2016); we applied a breakpoint analysis to the time-series of melt-out dates. This preliminary analysis points to a significant tipping point in 1988, which is consistent with regional-scale studies (Reid et al., 2016). At 2400 m asl, the melt-out date thus advanced on average from June 14 (1959-1988) to May 28 (1989-2016). At the same time, mean May temperatures increased from 1.7°C to 3.5°C. At 1800/2000m, a shift of 19 days is observed for the melt-out date and an increase of 25% in SFGDD is observed. As a consequence, climate-growth analyses were systematically performed separately for the subperiods 1959-1988 and 1989-2016.

Statistical analysis of climate-growth relationships

Structural Equation Models (SEMs, Grace, 2006; Kline, 2011) enable (i) decomposition of total effects into direct and indirect types, and (ii) comparison of alternative models using indices of goodness of fit (Kline, 2011; Mitchell, 1992). SEMs have been used in previous ecological studies to investigate e.g. the impacts of shrub expansion on species richness and plant diversity (Boscutti et al., 2018), the relation between climate and mountain plant productivity (Choler, 2015; Jonas et al., 2008; Madrigal-González et al., 2017, 2018) or the relation between tree-ring width and sea surface temperature in Mexican dry forests (Brienen et al., 2010). Although SEMs have been used quite rarely in dendroecology to date, they can indeed improve our understanding of the concurrent effects that snow cover climatic variables have on growth. The following two-step procedure was used to build models for each site: (Fig. 2):

(i) bootstrapped correlation functions (BCFs) between the detrended chronologies, mean monthly air temperature (°C), monthly precipitation sums (mm), melt-out dates, and SFGDD series were computed with the *Treeclim* package (Zang and Biondi, 2015) in R (R Core Team, 2016) to identify climate variables that are significantly correlated ($P < 0.05$) with radial growth. To identify direct and indirect drivers of radial growth, we also computed partial correlation functions (PCFs); and

(ii) SEMs were developed with the "*Lavaan*" package (Rosseel, 2012) in R. The structure of the hypothetical SEM path structure (see Fig. 2) requires the incorporation of available *a priori* knowledge (Pérez-de-Lis et al., 2016). In this study, direct effects are given as standardized path or partial regression coefficients. According to the hypothesis formulated in the introduction, we considered SFGDD as a direct driver of radial growth, while melt-out timing was incorporated as an indirect parameter through its mediating effect on growing season length. The latter parameters formed the backbone of the SEMs at each site, while additional climatic variables significantly correlated ($p<0.05$) with radial growth (steps 1-2) were added as explanatory variables. To derive comparable estimates, we standardized all quantitative predictors to a mean of zero and to a standard deviation of one. To prevent any effect of multicollinearity among explanatory variables, we used variance inflation factors (VIF). Collinearity was assessed with a cut-off value of 3 (Zuur et al., 2010). To compare the competing models, each model was first evaluated with the Akaike Information Criterion (AIC, Akaike, 1981) for which lower values correspond to more parsimonious models. We thereafter employed the Chi-square (χ^2) difference statistic to control the overall fit and to verify whether the model was consistent with the data covariance matrix (p cut-off ≥ 0.05) (Kline, 2011). In addition, we computed the CFI (Comparative Fit Index, Bentler, 1990) with a CFI cut-off $\geq$ 0.90. Assumptions of normality and homogeneity of variance were controlled for every endogenous variable in the SEMs using qq-plots and standardized residuals vs. fitted values plots (see Fig. S1 in supplementary material).

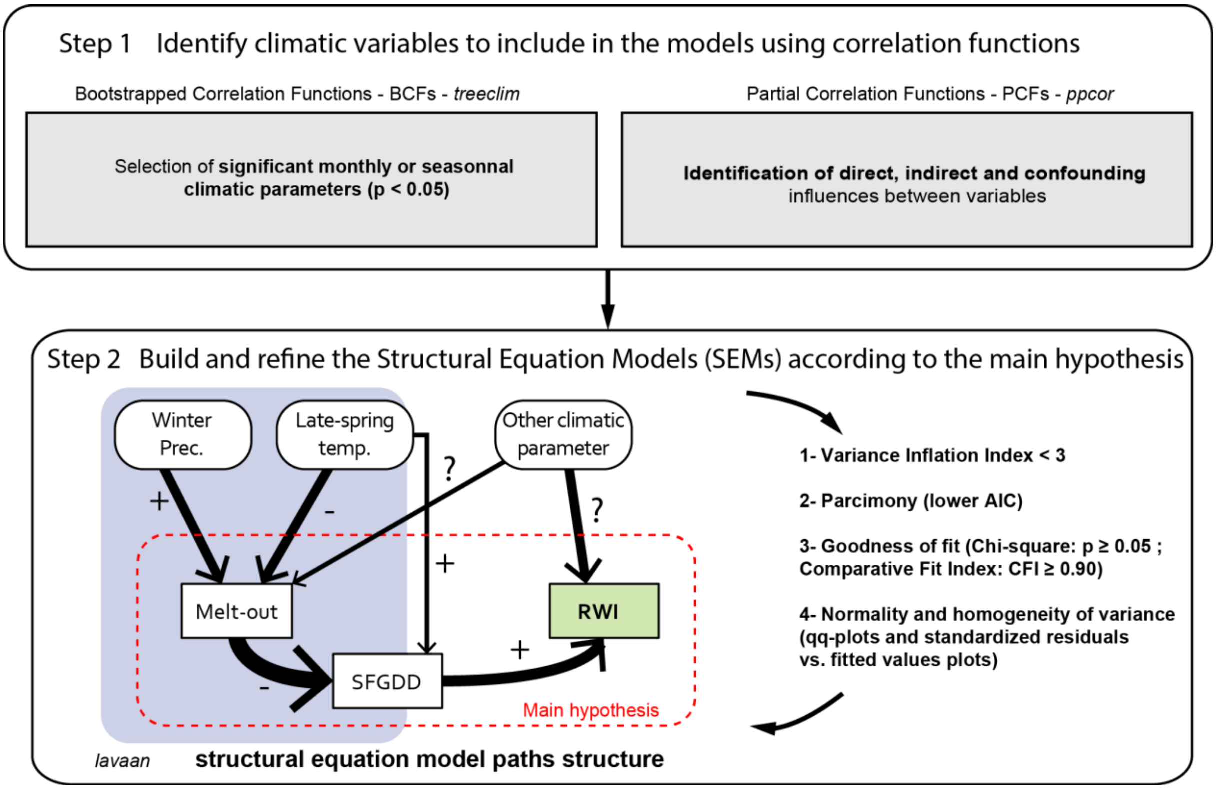

Figure 2: Diagram of the 2-step procedure adopted for the development of the Structural Equation Models (SEMs). First (step 1), Bootstrapped Correlation Functions (BCFs) are used to identify climatic variables that potentially have a direct or indirect effect on Ring-Width Indices (RWI) at the monthly or seasonal scales. Relationships with SFGDD and Melt-out dates were also tested. Climatic variables were then tested using Partial Correlation Functions (PCFs) for direct, indirect or confounding effects on RWI. Second (step 2), SEMs are built according to the main hypothesis (Melt-out timing → SFGDD → RWI) and with other climatic parameters selected in step 1. Collinearity, parsimony, goodness of fit and main assumptions (normality and homogeneity of variance) were controlled and the SEM structure was potentially refined.

Results

Chronology statistics

A total of 11, 24, and 14 *R. ferrugineum* individuals were included in the SAL1800 (1826-2016), SAL2000 (1821-2015) and CN2400 (1896-2016) chronologies, respectively (Fig. 3 A, B) corresponding to rejection rates (e.g. the percentage of misdated individuals) of 35, 33, and 48% of the samples. Cross-correlations between standardized chronologies over the period

1960-2016 yielded r values of 0.80 (SAL1800-SAL2000), 0.46 (SAL2000-CN2400) and 0.30 (SAL1800-CN2400). Wood productivity – estimated as the mean annual growth between cambial age 20 and 39 – was 0.17 mm at SAL1800, 0.16 mm at SAL2000, and thus significantly larger than the values obtained at CN2400 (0.12 mm, ANOVA $p<0.001$). Descriptive statistics computed for the detrended chronologies (Fig. 3B) are given in Table 1. Mean sensitivity values were comparable at SAL1800 (0.34) and CN2400 (0.31), but lower at SAL2000 (0.26). The highest inter-series correlations (Rbar = 0.41), EPS (0.94) and AC values (0.22) were observed at SAL2000. At SAL1800 and CN2400, lower Rbar and EPS values (slightly below the 0.85 threshold at CN2400) were found for the period covered by meteorological series (1959-2016), thereby pointing to higher inter-individual ring-width variability.

Table 1: Characteristics of *R. ferrugineum* raw ring-width chronologies: length, mean age, median ring-width. Statistics computed for detrended chronologies: standard deviation (Std. dev.), signal strength (Rbar and EPS, computed only from 1959 onwards), mean sensitivity (MS) and first order autocorrelation (AC).

	Raw ring-width chronologies				**Detrended ring-width chronologies**				
Chronology	First year	Last Year	Mean age	Median ring-width	Std. dev.	Mean Rbar (1959-2016)	Mean EPS (1959-2016)	MS	AC
SAL1800	1862	2016	81	0.171	0.281	0.321	0.86	0.338	0.136
SAL2000	1821	2015	86	0.159	0.246	0.412	0.94	0.257	0.221
CN2400	1896	2016	56	0.117	0.265	0.278	0.82	0.314	0.008

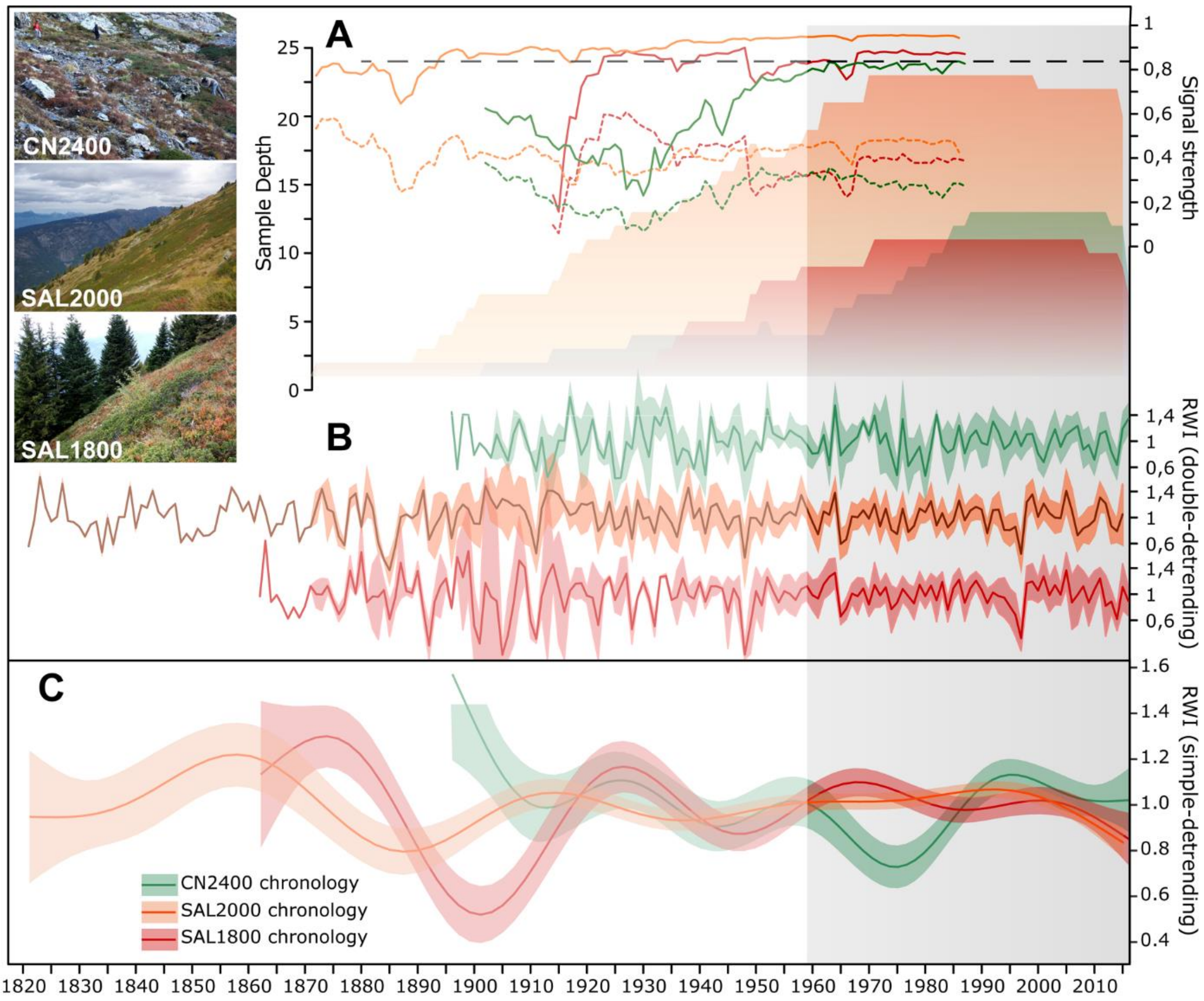

Figure 3: (A) Sample depth (colored areas) and running detrended chronologies signal strength: Expressed Population Signal (EPS, solid lines) and common variance between single growth-ring series in a chronology (Rbar, dotted lines) were computed using a 30-year moving window. Colored areas indicate sample depth. The EPS threshold (0.85) is shown by the black dotted line. (B) Standard growth-ring chronologies of *R. ferrugineum* with ribbons designating Ring-Width Indices (RWI) ± 1 SD. (C) Neg-Exp chronologies smoothed with a GAM-smoothing, ribbons indicate the 95% confidence intervals. The grey area corresponds to the period analyzed.

Bootstrapped correlation functions (BCFs) and partial correlation functions (PCFs)

Results from the bivariate bootstrapped correlation function analyses are summarized in Fig. 4. May temperatures (year N; r = 0.33, 0.34, 0.40 at 1800, 2000, and 2400 m asl, respectively, all with $p<0.05$) were the only statistically significant climatic driver of radial growth observed in all *R. ferrugineum* chronologies. More generally, positive correlations (albeit not significant) were observed between summer temperature of year N (June, July, and August) and radial growth at each site. Similar BCF profiles were observed at SAL1800 and SAL2000, characterized by positive significant correlations with September (year N-1) temperatures (r = 0.26 and r = 0.35, p<0.05) and April precipitation sums (r = 0.28, r = 0.28, p<0.05). By contrast, at CN2400, the response to fall (N-1) temperature was delayed to October (r = -0.28, p=0.06) and November (r = -0.30, p<0.05). The response of *R. ferrugineum* to snow melt-out date and SFGDD was particularly acute at 2400 m asl. The correlation between ring-width indices and SFGDD increased from low to high elevation sites, with r = 0.18 (p=0.18) at SAL1800, r = 0.28 (p<0.05) at SAL2000, and r = 0.51 at CN2400 (p<0.001). Radial growth also appeared to be more limited by melt-out date at CN2400 (r = -0.56, p<0.001) and winter precipitation (r = -0.41, p<0.01) as compared to r = 0 at SAL1800 (Fig. 4).

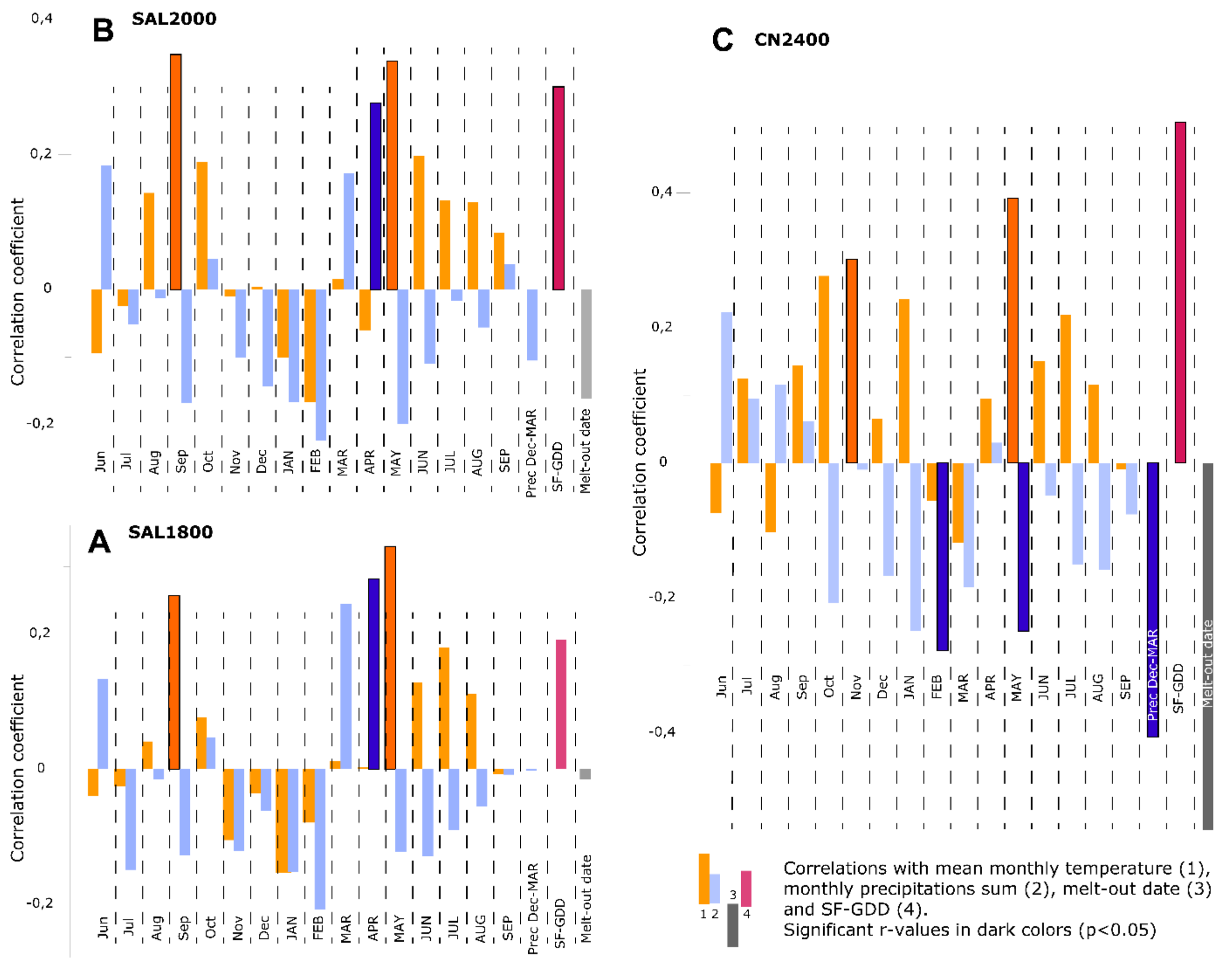

Figure 4: Monthly bootstrapped correlation functions (BCFs) analysis between *R. ferrugineum* radial growth chronologies at SAL1800 (A); SAL2000 (B); and CN2400 (C), monthly mean temperatures, monthly precipitation sums, previous December to current March precipitation sums (Prec dec-MAR), SFGDD and snow melt-out date for the period 1959–2016. Months of the year preceding ring formation

(N-1) are given with lowercase letters, and months of the year (N) of ring formation are shown with capital letters.

At our study sites, melt-out timing, late winter precipitation and May temperature are correlated, therefore partial correlations between tree-ring growth and the latter variables were performed. At CN2400, PCFs computed between radial growth, May temperature and precipitation or winter precipitation were not significant when melt-out timing was included as a control variable (Table 2). In other words, this indicates that the latter climatic variables have no impact on radial growth when melt-out-timing is held constant. Conversely, at SAL1800 and SAL2000, correlations between shrub chronologies, May temperature and March/April precipitation totals remain highly significant in the absence of melt-out timing fluctuations (Tab. 2). One can thus conclude that the correlations between our shrub ring width chronology and May temperature and late winter precipitation totals are 0.33 and 0.47 ($p<0.05$), respectively at SAL1800 if adjusted for the effects of melt-out timing. At SAL2000, the partial coefficients reveal the critical influence of May temperature ($r=0.32$, $p<0.05$) and Mar-Apr precipitation ($r=0.48$, $p<0.001$) on radial growth.

Table 2: Partial Correlations Functions (PCFs) and their significance computed between climatic parameters and ring width indices (RWI) at SAL1800, SAL2000 and CN24000 controlling for melt-out timing. Significant relationships ($p<0.05$) are given in bold. “na” means that the partial correlation was not computed, as no effect on radial growth was detected in the Bootstrapped Correlation Functions for the corresponding climatic variable.

	SAL1800		SAL2000		CN2400	
Effect	Corr.	Signif.	Corr.	Signif.	Corr.	Signif.
May temperature	**0.33**	**0.01**	**0.32**	**0.02**	0.03	0.84
March + April precipitation	**0.47**	**0.00**	**0.48**	**0.00**	na	na
Winter precipitation	na	na	na	na	-0.10	0.45
May precipitation	na	na	na	na	-0.08	0.56

Structural equation modeling

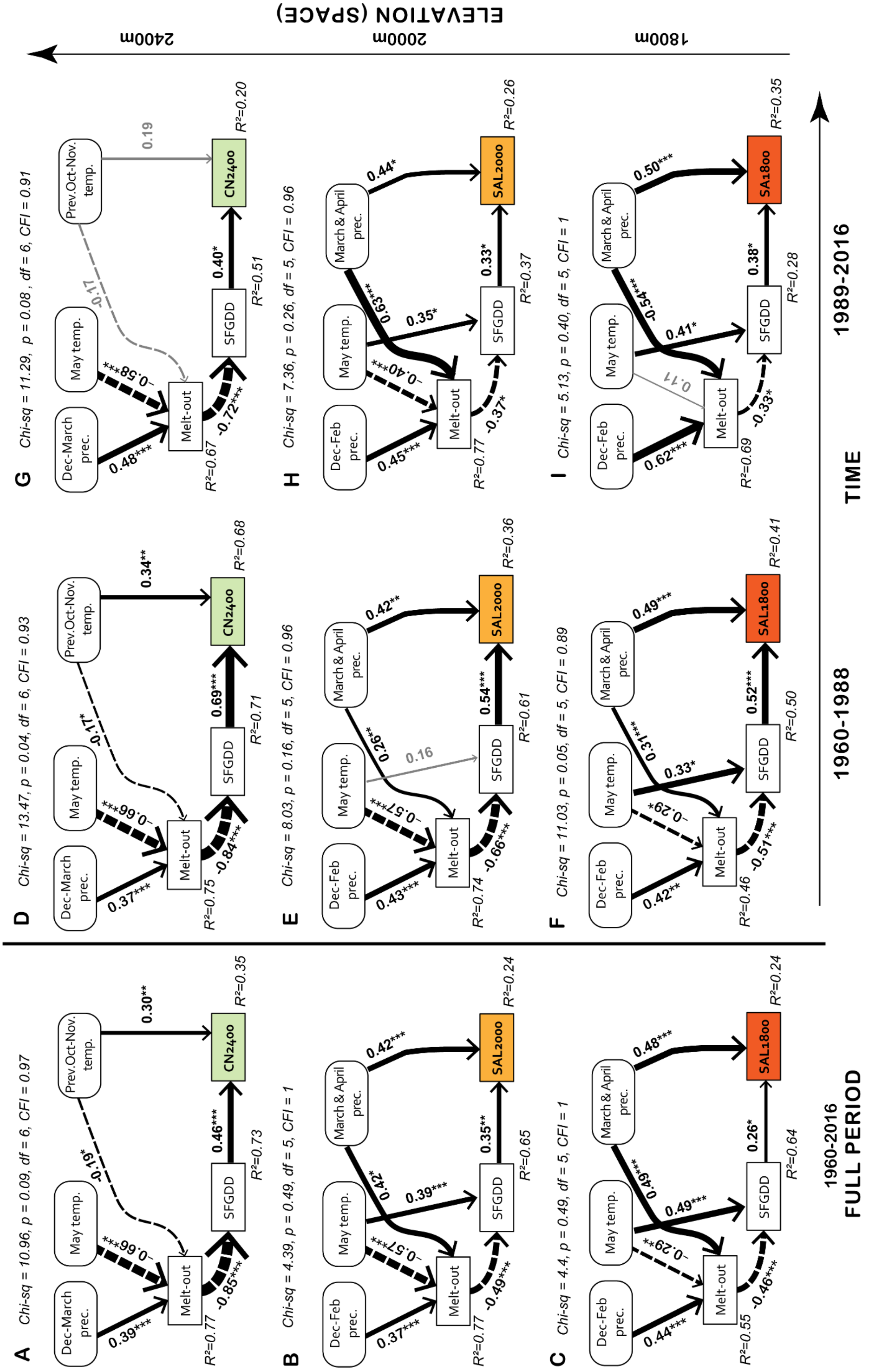
ELEVATION (SPACE)
2400m
2000m
1800m
TIME
1960-2016
FULL PERIOD
1960-1988
1989-2016
A
Chi-sq = 10.96, p = 0.09, df = 6, CFI = 0.97
B
Chi-sq = 4.39, p = 0.49, df = 5, CFI = 1
C
Chi-sq = 4.4, p = 0.49, df = 5, CFI = 1
D
Chi-sq = 13.47, p = 0.04, df = 6, CFI = 0.93
E
Chi-sq = 8.03, p = 0.16, df = 5, CFI = 0.96
F
Chi-sq = 11.03, p = 0.05, df = 5, CFI = 0.89
G
Chi-sq = 11.29, p = 0.08, df = 6, CFI = 0.91
H
Chi-sq = 7.36, p = 0.26, df = 5, CFI = 0.96
I
Chi-sq = 5.13, p = 0.40, df = 5, CFI = 1
Dec-March prec.
Dec-Feb prec.
May temp.
Prev.Oct-Nov. temp.
March & April prec.
Melt-out
SFGDD
CN2400
SAL2000
SAL1800
SA1800

Figure 5: Results of structural equation models (SEMs) exploring the effects of spring snow-cover duration (Melt-out) on Snow-Free Growing Degree Days (SFGDD), and the effects of SFGDD and other climatic parameters (March and April precipitation totals at SAL1800/2000, previous September temperature at SAL2000 and previous October-November temperature at CN2400) on shrub ring width indices (RWI) at different sites (A, D, G: 1800 m asl, SAL1800; B, E, H: 2000 m asl, SAL2000 and C, F, I: 2400 m asl, CN2400). SEMs were performed for the period 1960-2016 (A, B, C) and two sub-periods: 1960-1988 (D, E, F) and 1989-2016 (G, H, I). Winter precipitation totals and May temperature effects on Melt-out timing as well as the direct effect of May temperature on SFGDD are also represented. Colored boxes represent measured RWI, white boxes represent intermediate climate parameters and rounded white boxes represent monthly or seasonal meteorological data. Black solid (or dotted) arrows indicate unidirectional positive (negative) significant relationships (at $p<0.05$) among variables. Grey arrows indicate non-significant relationship ($p>0.05$). The thickness of the paths was scaled to the magnitude of the standardized regression coefficient (shown besides the arrows). Multiple R^2 are given next to the box of the respective response variable. Significance levels are denoted by *** ($p < 0.001$), ** ($p < 0.01$), * ($p < 0.05$). Chi-square and CFI values indicate goodness of fit.

Results from BCFs and PCFs were used to determine the direction and strength of correlations between climate variables and the shrub ring chronologies implemented in the path diagrams of each structural equation model over the period 1960-2016 (Figs. 5A-C). At each site, as stated in our initial hypotheses (Fig. 2), path diagrams were designed to disentangle the respective impacts of SFGDD, melt-out timing, winter precipitation and spring temperatures on shrub radial growth. In addition to the latter variables, fall temperatures (N-1, CN2400, SAL2000) and spring precipitation (SAL1800, SAL2000), significantly correlated to shrub ring records (BCFs), were added as direct predictor variables. SEMs computed for the periods 1960-2016 displayed Chi-square p-values above 0.05 and CFI higher than the 0.9 cut-off. At the three sites, the proportion of the variance in the dendrochronological series that could be explained by the climatic variables increased with elevation (R^2= 0.35, 0.24, 0.24 at CN2400, SAL2000 and SAL1800, respectively). However, the effect of SFGDD on shrub ring records increased from 0.26 standard deviation units as a result of change of one standard deviation in SFGDD at 1800 m ($p<0.05$) to 0.35 ($p<0.01$) at 2000 m and to 0.46 ($p<0.001$) at 2400 m asl. Significant relations between climatic variables and radial growth differed along the elevational gradient. At CN2400, SFGDD variability is the main driver of radial growth, which is significantly related to melt-out-timing (path coefficient of -0.85, $p<0.001$). Melt-out was in turn directly conditioned by May temperature (-0.66, p<0.001), winter precipitation (0.39, p<0.001) and – to a lesser extent – by previous late-autumn temperature (-0.19, p<0.05).

At SAL2000, SFGDD, spring precipitation and previous fall temperature show comparable, statistically significant impacts on shrub radial growth. Interannual variability of SFGDD remains dependent on melt-out timing but is also directly driven by May temperature (Fig. 5B). Finally, at 1800 m asl, the SEM differs from those obtained for the higher elevation sites. Albeit significantly related to radial growth at SAL1800, SFGDD is not the main driver for shrub ring width which appears to depend more strongly on March-April precipitation totals (0.48, p<0.001). At this elevation, SFGDD is driven by melt-out timing and May temperature (-0.46, p<0.001 and 0.49, p<0.001, respectively).

Stationarity of radial growth-climate relationships over time

To evaluate the stationarity and consistency of radial growth-climate relationships, SEMs were computed for the two sub-periods 1960-1988 and 1989-2016 (Fig. 5 D-I). The SEMs presented good overall performances by passing the goodness of fit cutoffs of Chi-square p>0.05 and CFI >0.90 except for the SEMs computed at CN2400 and SAL1800 for the period 1960-1988 (χ^2 = 13.47, p=0.04, CFI = 0.93 at CN2400 and χ^2 = 11.03, p=0.05, CFI = 0.89 at SAL1800).

Strikingly, we observe a loss of the explanatory powers of the SEMs for the recent period, especially at CN2400 where the amount of variance in radial growth explained by climatic variables decreased from 0.69 for the period 1960-1988 to 0.20 between 1989 and 2016. For both subperiods, the dependence of radial growth on SFGDD thus decreased from 0.69 (p<0.001) to 0.40 (p<0.05), from 0.54 (p<0.001) to 0.33 (p<0.05), and from 0.52 (p<0.001) to 0.38 (p<0.05) at 2400, 2000, and 1800 m asl, respectively. In addition, the models illustrate nicely that the dependence of SFGDD on melt-out dates and May temperatures remain highly significant (p<0.001) at CN2400, whereas their influence strongly decreased at SAL2000 and

SAL1800 after 1988. Similarities exist between the SEM computed at SAL2000 for the period 1960-1988 and at CN2400 for the period 1989-2016 (Fig. 5 E, G), especially with respect to the correlations between May temperatures, melt-out timing, SFGDD and radial growth. Similarly, comparable impacts of winter precipitations and May temperatures on melt-out dates were observed in Fig. 5F and 5H. This evolution suggests a 200-400 m shift of the climatic conditions and, to a lesser extent, of radial growth response to climate over the last 30 years.

Discussion

In this paper, we disentangled the impact of recent climate change, especially of earlier snow melt-out, on radial growth in the widespread mountain shrub species *Rhododendron ferrugineum* by sampling a total of 80 stems along an elevation gradient. The three multi-decadal growth-ring chronologies developed from individuals sampled at 1800, 2000, and 2400 m asl (referred to as SAL1800, SAL2000, and CN2400) provide a unique perspective on mountain shrub responses to climate variability in the context of recent climate changes (Myers-Smith et al., 2015). We used Structural Equation Models (SEMs), rarely used in dendroecological studies so far, to disentangle direct and indirect drivers of radial growth. Our results clearly demonstrate an elevation-dependent response of *R. ferrugineum* to snow cover duration and provide evidence for a divergence of radial growth responses to climate during recent decades, given that climate-growth correlations have weakened since 1988. This study also benefits from the hourly-resolution of meteorological as well as snow series from the SAFRAN-Crocus dataset. The latter data, available at the elevations of the three study plots for the period 1960-2017, are of a precision that is only rarely equaled in any previously published alpine or arctic dendroecological study.

Radial growth responses along the snow melt-out timing gradient

At CN2400, results support the initial hypothesis that the amount of growing degree days during the snow-free period (SFGDD) would impact *R. ferrugineum* radial growth strongly whereas melt-out dates would act only as an indirect limiting factor on radial growth by conditioning the length of the growing season. Results from SEMs show that SFGDD – controlled by melt out dates – explained about 46% of radial growth variability over the period 1960-2016 and about 70% of the variability between 1960 and 1988. At this elevation, the growing season is short (85 days on average prior to August 31) and SFGDD totals are low (823°C on average for the period 1959-2016). Snowmelt frequently occurs between early and mid-June and coincides with peak annual temperatures and photoperiod, i.e. when the carbon gain of a single bright day is at its maximum. Consequently, any variation in melt-out dates, even by a few days, can affect SFGDD totals strongly, and can thus also explain the strong correlation between both variables ($r = -0.85$, $p<0.001$).

R. ferrugineum is an evergreen shrub that has developed an opportunistic growth strategy, able to photosynthesize within two hours after snow removal (Larcher and Siegwolf, 1985). We can therefore reasonably assume that the species will also benefit from an earlier growing season, consistent with the correlation between SFGDD and radial growth. Our results are in line with numerous studies from Arctic and Alpine environments, which demonstrated that the accumulation of temperature above a certain threshold is a key factor driving growth through cell division and differentiation (Hoch, 2015; Körner, 2003; Wheeler et al., 2016; Wipf, 2010) and phenological transitions (Kudo and Suzuki, 1999; Molau et al., 2005). Results are also consistent with (i) dendrochronological studies that demonstrated the negative effect of snowpack duration on radial growth at the upper shrub limit in the Alps (Carrer et al., 2019; Francon et al., 2017; Pellizzari et al., 2014) and (ii) manipulation experiments (Stinson, 2005; Wheeler et al., 2016) showing increased productivity in case of artificial snow removal at sites where melt-out dates occurred after late-May (Wipf and Rixen, 2010). Results from the Alps differ from the wealth of studies in the Arctic, where a positive effect of snowpack was highlighted. We can explain this discrepancy by the fact that, in the Arctic, the positive winter precipitation effect is mostly related to snowpack thermal insulation, which protects plants from the harsh external conditions but also promotes higher winter soil surface temperatures with greater decomposition and nutrient release (Chapin, 2005; Hallinger et al., 2010). Furthermore, Alpine snowpack tends to be deeper and winter temperatures milder compared to the Arctic, and accordingly soil temperatures less sensitive to a slight change in snow accumulation. In the context of our study sites, root and vegetative shrub tissues are likely more protected from persistent negative temperatures in the Alps than in the Arctic (Domine et al., 2016; Ernakovich et al., 2014).

By contrast, at the lower sites (SAL1800, SAL2000), our results indicate that the weaker effects of (i) snow cover duration on SFGDD and (ii) SFGDD on ring width can be explained by earlier melt-out dates, occurring at these elevations between early and mid-May, when daily temperatures (4.9°C and 6.4 °C in May on average for the 1960-2016 period at 2000 and 1800m asl, respectively) and solar radiation have not yet attained peak values and are insufficient for shrub growth. In addition, SFGDD at SAL1800 and SAL2000 (1316°C on average) are significantly higher than those estimated at CN2400 and thus certainly less constraining for plants to complete the phenological cycle and a complete carbon storage at the end of the growing season. These hypotheses are consistent with experiments showing neutral to negative impacts of early (i.e. late-April) artificial snow removal (Dorrepaal et al., 2006; Wipf et al., 2006, 2009) at sites where natural early melt-out date would occur before mid-May. Wipf et al. (2009) found a general decrease in shoot growth in mountain shrub species (*Empetrum nigrum*, *Vaccinium myrtillus* and *V. uliginosum*) under earlier melt-out dates due to higher frost exposure. In the specific case of *R. ferrugineum*, Malfasi and Cannone (2020) found that the recruitment rate was favored by prolonged snow cover occurrence. In our case, the positive effect of a longer growing season on radial growth can be similarly offset by the detrimental impact of spring frost (Choler, 2015; Jonas et al., 2008) or drought (Wheeler et al., 2016). Accordingly, we hypothesize that the positive correlations observed between low-elevation chronologies and March-April precipitation sums could either reflect (i) the positive effect of early spring precipitation on nutrient supply at the beginning of the growing season by enhancing decomposition and nitrogen mineralization right after snow melt-out (Baptist et al., 2010; Ernakovich et al., 2014) or (ii) the protective effect of late snowfalls against late frost (Choler, 2015; Jonas et al., 2008), irradiation (Neuner et al., 1999) or limited drought stress during the subsequent growing season (Buchner and Neuner, 2003; Daniels and Veblen, 2004).

In the case of the Taillefer massif, a detailed analysis of meteorological conditions and radial growth in 1997 is relevant in order to illustrate the detrimental effects of late frost. According to the SAFRAN-Crocus reanalysis, melt-out occurred on approximately April 14 at lower elevations (SAL1800 and SAL2000,) and on May 31 at CN2400. At lower elevations, spring 1997 was the coldest since 1959 at the ground level. Immediately after melt-out, two cold episodes with two extreme freezing periods occurred between April 14 and 24 and between May 6 and 9. Ground level temperatures reached their absolute minimum on April 17 at -7.3°C. The same year, a majority of *R. ferrugineum* individuals from the two lower elevation sites formed extremely narrow rings, whereas no significant growth reduction was observed at 2400 m asl where plants were still under snow. This suggests that very low productivity at SAL1800 and SAL2000 is linked to cellular damage associated with intense late frost which likely damaged fine roots, leaves, buds, and the cambium (Inouye, 2000; Wipf et al., 2006; Wipf and Rixen, 2010). However, the absence of other events comparable to 1997 in meteorological or ring width series does not allow inference of robust relationships between late frost and radial growth. Here, experimental testing using ecophysiological monitoring could be used to further explore the effects of frost events on radial growth (Charrier et al., 2017).

Climate warming, trend analysis and the divergence problem

Our study demonstrates diverging effects of growing season length and snowmelt timing on radial growth along the elevational gradient. At CN2400, the decadal growth trend follows that of SFGDD, in line with findings from the Arctic (Myers-Smith et al., 2015a). In addition, at lower elevation sites, our results also point to a divergence of radial growth as radial growth did not track the SFGDD increase during more recent decades. These results concur with the growth decline detected since the 1990s in shrub rings of *B. nana* and *S. glauca* from Western Greenland, where reduced ring width was attributed to increasing moisture limitation (Gamm et al., 2018). In the Taillefer massif, a weakening of the climatic signal is observed in shrub-ring chronologies after 1988, a year that can be considered as a tipping point in the meteorological series. Interestingly, comparable trends were reported for *B. nana* and *E. hermaphroditum* in the central Norwegian Scandes, where the positive influence of summer conditions was replaced by a negative response to May temperatures, over the last decades (Weijers et al., 2018a, 2018b). These findings echo the "divergence problem" reported in trees growing at circumpolar, northern latitudes (Briffa et al., 1998; D'Arrigo et al., 2008; Driscoll, 2005) and high-elevation sites (Büntgen et al., 2006, 2008). This body of evidence suggests more complex and nonlinear growth responses of trees to a changing climate, thereby leading to a decrease in year-to-year sensitivity of tree growth (i.e. "non-stationarity") in previously temperature-limited sites (D'Arrigo et al., 2008; Vaganov et al., 1999; Wilmking, 2005; Wilmking et al., 2020). Potential causes for this divergence include warming-induced thresholds of tree growth (D'Arrigo et al., 2004; Jochner et al., 2018), limitation of growth by nutrient availability (Fajardo and Piper, 2017) or drought stress (Büntgen et al., 2006) or interactions between these factors. In the case of low-stature alpine vegetation, frost damage (Phoenix and Bjerke, 2016; Treharne et al., 2019) could also be assumed as a cause divergence, and merits further investigation.

Conclusion

In this paper, we analyze annually resolved, statistically solid multi-decadal chronologies of 49 *R. ferrugineum* shrubs sampled along an elevational gradient in the French Alps. Results show that a clear, elevation-dependent climatic signal exists in the growth-ring series covering the period 1959-2016. Comparison of the SEMs along the elevational gradient shows that SFGDD and, by extension, melt-out dates are the main drivers of radial growth at 2400 m asl. By contrast, at lower elevations, melt-out dates have a limited effect on SFGDD, as the latter only barely limit radial growth. In addition, meteorological and snowpack series from the model SAFRAN-Crocus point to a breakpoint in 1988. In fact, since the late 1980s, melt-out dates have advanced by an average of 17 to 19 days depending on elevation. Since 1988, our study provides evidence of a recent divergence in radial growth, insofar as the increase in SFGDD results in a weakening of the climatic signal in shrub ring-width chronologies, similar to the divergence observed in trees at circumpolar and alpine sites. Moreover, at lower elevations (1800 and 2000 m asl), an extremely narrow ring was formed in 1997 following a late frost event. Albeit unique in the dendrochronological series, it illustrates the potential detrimental effects of early melt-out dates on productivity. Accordingly, 1997 might well be an example of extreme events that can be expected to become more frequent in a warmer climate. This non-stationarity of climate-growth relationships suggests strong threshold effects in terms of temperature and melt-out timing in a context of global warming.

This study shows that *R. ferrugineum* is particularly sensitive to local meteorological conditions such as snow cover or frost events. For this reason and given its large occurrence above the treeline in the Alps and Pyrenees (Francon et al., 2017; Gracia et al., 2007), we believe that this species represents a valuable dendroecological indicator to document the response of alpine vegetation to global warming over the last centuries. As such, *R. ferrugineum* could be used easily to complement *Juniperus nana* in future dendroecological studies, even more so as both species are characterized by a wide distribution above treeline and a life span of more than a century (Carrer et al., 2019; Pellizzari et al., 2014, 2016). Yet, unlike *J. nana*, whose radial growth is mainly driven by regional climate variability (Carrer et al., 2019), *R. ferrugineum* seems to be very sensitive to fine-scale climatic variations induced by topography.

To further improve our understanding of the processes governing shrub growth in mountain environments and to precisely define the values of the above-mentioned climatic thresholds, including the potential impact of extreme climatic events, we recommend that future research be directed in two directions. Firstly, more populations growing in contrasting topoclimatic situations across the Alps should be sampled and compared with topoclimatic data. Secondly, we plead for future work to combine field-based eco-physiological and microclimatic monitoring (see e.g. Charrier et al. 2017), with remote sensing of landscape-scale vegetation dynamics in alpine regions (see e.g. Carlson et al., 2017; Bayle et al. (2019).

Acknowledgments

This research was supported by the program ProXyCliM (2016–2017) funded by the CNRS (Mission interdisciplinarité - RNMSH) and by the french national grant EC2CO-Biohefect/Ecodyn//Dril/MicrobiEen, SNOWSHRUB. We wish to thank all who contributed to the meteorological series data used in the analyses, especially Carlo Maria Carmagnola (Météo-France - CNRS, CNRM, CEN). We are particulartly grateful to Brigitte Girard (INRA, PIAF) for her much appreciated help during the tedious phase of the laboratory. We acknowledge Olivier Voldoire (GEOLAB, CNRS) for technical support. Rhododendron shrubs were sampled with the help of Séverine Finet, and Robin Mainieri. We are also grateful to Frida Piper and Jaime Madrigal González for insightful feedback on the manuscript. CNRM/CEN, Irstea/ETNA and LECA are part of LabEX OSUG@2020.

References

Ackerman D, Griffin D, Hobbie SE, Finlay JC. 2017. Arctic shrub growth trajectories differ across soil moisture levels. Global Change Biology **23** : 4294–4302. DOI: 10.1111/gcb.13677

Akaike H. 1981. Likelihood of a model and information criteria. Journal of Econometrics **16** : 3–14. DOI: 10.1016/0304-4076(81)90071-3

Anthelme F, Villaret J-C, Brun J-J. 2007. Shrub encroachment in the Alps gives rise to the convergence of sub-alpine communities on a regional scale. Journal of Vegetation Science **18** : 355–362. DOI: 10.1111/j.1654-1103.2007.tb02547.x

Baptist F, Yoccoz NG, Choler P. 2010. Direct and indirect control by snow cover over decomposition in alpine tundra along a snowmelt gradient. Plant and Soil **328** : 397–410. DOI: 10.1007/s11104-009-0119-6

Bär A, Bräuning A, Löffler J. 2006. Dendroecology of dwarf shrubs in the high mountains of Norway – A methodological approach. Dendrochronologia **24** : 17–27. DOI: 10.1016/j.dendro.2006.05.001

Bär A, Pape R, Bräuning A, Löffler J. 2008. Growth-ring variations of dwarf shrubs reflect regional climate signals in alpine environments rather than topoclimatic differences. Journal of Biogeography **35** : 625–636. DOI: 10.1111/j.1365-2699.2007.01804.x

Bayle A, Carlson B, Thierion V, Isenmann M, Choler P. 2019. Improved Mapping of Mountain Shrublands Using the Sentinel-2 Red-Edge Band. Remote Sensing **11** : 2807. DOI: 10.3390/rs11232807

Beniston M et al. 2018. The European mountain cryosphere: a review of its current state, trends, and future challenges. The Cryosphere **12** : 759–794. DOI: 10.5194/tc-12-759-2018

Bentler P. 1990. Comparative fit indexes in structural models. Psychological Bulletin **107** : 228–246.

Bjorkman AD et al. 2018. Plant functional trait change across a warming tundra biome. Nature DOI: 10.1038/s41586-018-0563-7 [online] Available from: http://www.nature.com/articles/s41586-018-0563-7 (Accessed 2 October 2018)

Bjorkman AD et al. 2020. Status and trends in Arctic vegetation: Evidence from experimental warming and long-term monitoring. Ambio **49** : 678–692. DOI: 10.1007/s13280-019-01161-6

Blok D, Sass-Klaassen U, Schaepman-Strub G, Heijmans MMPD, Sauren P, Berendse F. 2011. What are the main climate drivers for shrub growth in Northeastern Siberian tundra? Biogeosciences **8** : 1169–1179. DOI: 10.5194/bg-8-1169-2011

Boscutti F, Casolo V, Beraldo P, Braidot E, Zancani M, Rixen C. 2018. Shrub growth and plant diversity along an elevation gradient: Evidence of indirect effects of climate on alpine ecosystems. Carcaillet C (ed). PLOS ONE **13** : e0196653. DOI: 10.1371/journal.pone.0196653

Brienen RJW, Lebrija-Trejos E, Zuidema PA, Martínez-Ramos M. 2010. Climate-growth analysis for a Mexican dry forest tree shows strong impact of sea surface temperatures and predicts future growth declines: CLIMATE-GROWTH ANALYSIS OF A DRY FOREST TREE. Global Change Biology **16** : 2001–2012. DOI: 10.1111/j.1365-2486.2009.02059.x

Briffa KR, Schweingruber FH, Jones PD, Osborn TJ, Shiyatov SG, Vaganov EA. 1998. Reduced sensitivity of recent tree-growth to temperature at high northern latitudes. Nature **391** : 678–682.

Buchner O, Neuner G. 2003. Variability of Heat Tolerance in Alpine Plant Species Measured at Different Altitudes. Arctic, Antarctic, and Alpine Research **35** : 411–420. DOI: 10.1657/1523-0430(2003)035[0411:VOHTIA]2.0.CO;2

Buchwal A, Rachlewicz G, Fonti P, Cherubini P, Gärtner H. 2013. Temperature modulates intra-plant growth of Salix polaris from a high Arctic site (Svalbard). Polar Biology **36** : 1305–1318. DOI: 10.1007/s00300-013-1349-x

Büntgen U, Frank D, Wilson R, Carrer M, Urbinati C, Esper J. 2008. Testing for tree-ring divergence in the European Alps. Global Change Biology **14** : 2443–2453. DOI: 10.1111/j.1365-2486.2008.01640.x

Büntgen U, Frank DC, Nievergelt D, Esper J. 2006. Summer Temperature Variations in the European Alps, A.D. 755–2004. Journal of Climate **19** : 5606–5623. DOI: 10.1175/JCLI3917.1

Cannone N, Sgorbati S, Guglielmin M. 2007. Unexpected impacts of climate change on alpine vegetation. Frontiers in Ecology and the Environment **5** : 360–364. DOI: 10.1890/1540-9295(2007)5[360:UIOCCO]2.0.CO;2

Carlson BZ, Corona MC, Dentant C, Bonet R, Thuiller W, Choler P. 2017. Observed long-term greening of alpine vegetation—a case study in the French Alps. Environmental Research Letters **12** : 114006. DOI: 10.1088/1748-9326/aa84bd

Carrer M, Pellizzari E, Prendin AL, Pividori M, Brunetti M. 2019. Winter precipitation - not summer temperature - is still the main driver for Alpine shrub growth. Science of The Total Environment **682** : 171–179. DOI: 10.1016/j.scitotenv.2019.05.152

Chapin FS. 2005. Role of Land-Surface Changes in Arctic Summer Warming. Science **310** : 657–660. DOI: 10.1126/science.1117368

Charrier G, Nolf M, Leitinger G, Charra-Vaskou K, Losso A, Tappeiner U, Améglio T, Mayr S. 2017. Monitoring of Freezing Dynamics in Trees: A Simple Phase Shift Causes Complexity. Plant Physiology **173** : 2196–2207. DOI: 10.1104/pp.16.01815

Chen I-C, Hill JK, Ohlemuller R, Roy DB, Thomas CD. 2011. Rapid Range Shifts of Species Associated with High Levels of Climate Warming. Science **333** : 1024–1026. DOI: 10.1126/science.1206432

Choler P. 2015. Growth response of temperate mountain grasslands to inter-annual variations in snow cover duration. Biogeosciences **12** : 3885–3897. DOI: 10.5194/bg-12-3885-2015

Cook ER. 1987. The decomposition of tree-ring series for environmental studies. Tree Ring Bulletin **47** : 37–59.

Cook ER, Kairiukstis LA (eds). 1990. Methods of Dendrochronology . Springer Netherlands: Dordrecht

Cook ER, Peters K. 1981. The smoothing spline: a new approach to standardizing forest interior tree-ring width series for dendroclimatic studies. Tree Ring Bulletin **41** : 45–53.

Daniels LD, Veblen T. 2004. Spatiotemporal Influences of Climate on Altitudinal Treeline in Northern Patagonia. Ecology **85** : 1284–1296.

D'Arrigo R, Kaufmann RK, Davi N, Jacoby GC, Laskowski C, Myneni RB, Cherubini P. 2004. Thresholds for warming-induced growth decline at elevational tree line in the Yukon Territory, Canada: THRESHOLDS FOR WARMING-INDUCED GROWTH DECLINE. Global Biogeochemical Cycles **18** : n/a-n/a. DOI: 10.1029/2004GB002249

D'Arrigo R, Wilson R, Liepert B, Cherubini P. 2008. On the 'Divergence Problem' in Northern Forests: A review of the tree-ring evidence and possible causes. Global and Planetary Change **60** : 289–305. DOI: 10.1016/j.gloplacha.2007.03.004

Dedieu J-P, Carlson B, Bigot S, Sirguey P, Vionnet V, Choler P. 2016. On the Importance of High-Resolution Time Series of Optical Imagery for Quantifying the Effects of Snow Cover Duration on Alpine Plant Habitat. Remote Sensing **8** : 481. DOI: 10.3390/rs8060481

Doche B, Franchini S, Pornon A, Lemperiere G. 2005. Changes of Humus Features along with a Successional Gradient of Rhododendron ferrugineum (L.) Populations (Subalpine Level, Northwestern Alps, France). Arctic, Antarctic, and Alpine Research **37** : 454–464. DOI: 10.1657/1523-0430(2005)037[0454:COHFAW]2.0.CO;2

Dolezal J et al. 2016. Vegetation dynamics at the upper elevational limit of vascular plants in Himalaya. Scientific Reports **6** DOI: 10.1038/srep24881 [online] Available from: http://www.nature.com/articles/srep24881 (Accessed 7 December 2018)

Domine F, Barrere M, Morin S. 2016. The growth of shrubs on high Arctic tundra at Bylot Island: impact on snow physical properties and permafrost thermal regime. Biogeosciences **13** : 6471–6486. DOI: 10.5194/bg-13-6471-2016

Dorrepaal E, Aerts R, Cornelissen JHC, Van Logtestijn RSP, Callaghan TV. 2006. Sphagnum modifies climate-change impacts on subarctic vascular bog plants. Functional Ecology **20** : 31–41. DOI: 10.1111/j.1365-2435.2006.01076.x

Driscoll WW. 2005. Divergent tree growth response to recent climatic warming, Lake Clark National Park and Preserve, Alaska. Geophysical Research Letters **32** DOI: 10.1029/2005GL024258 [online] Available from: http://doi.wiley.com/10.1029/2005GL024258 (Accessed 29 May 2018)

Dullinger S, Dirnböck T, Grabherr G. 2003. Patterns of Shrub Invasion into High Mountain Grasslands of the Northern Calcareous Alps, Austria. Arctic, Antarctic, and Alpine Research **35** : 434–441. DOI: 10.1657/1523-0430(2003)035[0434:POSIIH]2.0.CO;2

Durand Y, Giraud G, Laternser M, Etchevers P, Mérindol L, Lesaffre B. 2009a. Reanalysis of 47 Years of Climate in the French Alps (1958–2005): Climatology and Trends for Snow Cover. Journal of Applied Meteorology and Climatology **48** : 2487–2512. DOI: 10.1175/2009JAMC1810.1

Durand Y, Laternser M, Giraud G, Etchevers P, Lesaffre B, Mérindol L. 2009b. Reanalysis of 44 Yr of Climate in the French Alps (1958–2002): Methodology, Model Validation, Climatology, and Trends for Air Temperature and Precipitation. Journal of Applied Meteorology and Climatology **48** : 429–449. DOI: 10.1175/2008JAMC1808.1

Elmendorf SC et al. 2012. Plot-scale evidence of tundra vegetation change and links to recent summer warming. Nature Climate Change **2** : 453–457. DOI: 10.1038/nclimate1465

Elmendorf SC et al. 2015. Experiment, monitoring, and gradient methods used to infer climate change effects on plant communities yield consistent patterns. Proceedings of the National Academy of Sciences **112** : 448–452. DOI: 10.1073/pnas.1410088112

Elsen PR, Tingley MW. 2015. Global mountain topography and the fate of montane species under climate change. Nature Climate Change **5** : 772–776. DOI: 10.1038/nclimate2656

Ernakovich JG, Hopping KA, Berdanier AB, Simpson RT, Kachergis EJ, Steltzer H, Wallenstein MD. 2014. Predicted responses of arctic and alpine ecosystems to altered seasonality under climate change. Global Change Biology **20** : 3256–3269. DOI: 10.1111/gcb.12568

Escaravage N, Pornon A, Doche B, Till-Bottraud I. 1997. Breeding system in an alpine species: *Rhododendron ferrugineum* L. (Ericaceae) in the French northern Alps. Canadian Journal of Botany **75** : 736–743. DOI: 10.1139/b97-084

Escaravage N, Questiau S, Pornon A, Doche B, Taberlet P. 1998. Clonal diversity in a Rhododendron ferrugineum L.(Ericaceae) population inferred from AFLP markers. Molecular ecology **7** : 975–982.

Fajardo A, Piper FI. 2017. An assessment of carbon and nutrient limitations in the formation of the southern Andes tree line. McGlone M (ed). Journal of Ecology **105** : 517–527. DOI: 10.1111/1365-2745.12697

Forbes BC, Fauria MM, Zetterberg P. 2010. Russian Arctic warming and 'greening' are closely tracked by tundra shrub willows. Global Change Biology **16** : 1542–1554. DOI: 10.1111/j.1365-2486.2009.02047.x

Francon L, Corona C, Roussel E, Lopez Saez J, Stoffel M. 2017. Warm summers and moderate winter precipitation boost Rhododendron ferrugineum L. growth in the Taillefer massif (French Alps). Science of The Total Environment **586** : 1020–1031. DOI: 10.1016/j.scitotenv.2017.02.083

Franklin RS. 2013. Growth response of the alpine shrub, Linanthus pungens, to snowpack and temperature at a rock glacier site in the eastern Sierra Nevada of California, USA. Quaternary International **310** : 20–33. DOI: 10.1016/j.quaint.2012.07.018

Fritts HC. 1976. Tree rings and climate . Academic Press: London ; New York

Gamm CM, Sullivan PF, Buchwal A, Dial RJ, Young AB, Watts DA, Cahoon SMP, Welker JM, Post E. 2018. Declining growth of deciduous shrubs in the warming climate of continental western Greenland. Cornelissen H (ed). Journal of Ecology **106** : 640–654. DOI: 10.1111/1365-2745.12882

Gerdol R, Siffi C, Iacumin P, Gualmini M, Tomaselli M. 2013. Advanced snowmelt affects vegetative growth and sexual reproduction of *Vaccinium myrtillus* in a sub-alpine heath. Collins B (ed). Journal of Vegetation Science **24** : 569–579. DOI: 10.1111/j.1654-1103.2012.01472.x

Gottfried M et al. 2012. Continent-wide response of mountain vegetation to climate change. Nature Climate Change **2** : 111–115. DOI: 10.1038/nclimate1329

Grabherr G, Gottfried M, Pauli H. 1994. Climate effects on mountain plants. Nature **369** : 448–448. DOI: 10.1038/369448a0

Grace JB. 2006. Structural equation modeling and natural systems . Cambridge University Press: Cambridge, UK ; New York

Gracia M, Montané F, Piqué J, Retana J. 2007. Overstory structure and topographic gradients determining diversity and abundance of understory shrub species in temperate forests in central Pyrenees (NE Spain). Forest Ecology and Management **242** : 391–397. DOI: 10.1016/j.foreco.2007.01.056

Hallinger M, Manthey M, Wilmking M. 2010. Establishing a missing link: warm summers and winter snow cover promote shrub expansion into alpine tundra in Scandinavia. New Phytologist **186** : 890–899. DOI: 10.1111/j.1469-8137.2010.03223.x

Hantel M, Ehrendorfer M, Haslinger A. 2000. Climate sensitivity of snow cover duration in Austria. International Journal of Climatology **20** : 615–640. DOI: 10.1002/(SICI)1097-0088(200005)20:6<615::AID-JOC489>3.0.CO;2-0

Hantel M, Maurer C, Mayer D. 2012. The snowline climate of the Alps 1961–2010. Theoretical and Applied Climatology **110** : 517–537. DOI: 10.1007/s00704-012-0688-9

Hantemirov RM, Gorlanova LA, Shiyatov SG. 2000. Pathological tree-ring structures in Siberian juniper (juniperus sibirica burgsd.) and their use for reconstructing extreme climatic events. Russian Journal of Ecology **31** : 167–173. DOI: 10.1007/BF02762816

Hoch G. 2015. Carbon Reserves as Indicators for Carbon Limitation in Trees. In Progress in Botany , Lüttge U and Beyschlag W (eds). Springer International Publishing: Cham; 321–346. [online] Available from: http://link.springer.com/10.1007/978-3-319-08807-5_13 (Accessed 13 June 2018)

Hollesen J, Buchwal A, Rachlewicz G, Hansen BU, Hansen MO, Stecher O, Elberling B. 2015. Winter warming as an important co-driver for *Betula nana* growth in western Greenland during the past century. Global Change Biology **21** : 2410–2423. DOI: 10.1111/gcb.12913

Holmes RL. 1994. Dendrochronology Program Library User's Manual . Laboratory of Tree-Ring Research, University of Arizona: Tucson, Arizona

Inouye DW. 2000. The ecological and evolutionary significance of frost in the context of climate change. Ecology Letters **3** : 457–463. DOI: 10.1046/j.1461-0248.2000.00165.x

Jochner M, Bugmann H, Nötzli M, Bigler C. 2018. Tree growth responses to changing temperatures across space and time: a fine-scale analysis at the treeline in the Swiss Alps. Trees **32** : 645–660. DOI: 10.1007/s00468-017-1648-x

Jonas T, Rixen C, Sturm M, Stoeckli V. 2008. How alpine plant growth is linked to snow cover and climate variability. Journal of Geophysical Research **113** DOI: 10.1029/2007JG000680 [online] Available from: http://doi.wiley.com/10.1029/2007JG000680 (Accessed 12 June 2018)

Kline RB. 2011. Principles and practice of structural equation modeling . 3rd ed. Guilford Press: New York

Kolishchuk V. 1990. Dendroclimatological study of prostrate woody plant. In Methods of Dendrochronology, Applications in the Environmental Sciences , . Springer Netherlands: Dordrecht; 51–55.

Körner C. 2003. Alpine plant life: functional plant ecology of high mountain ecosystems . 2nd ed. Springer: Berlin ; New York

Kudo G, Suzuki S. 1999. Flowering phenology of alpine plant communities along a gradient of snowmelt timing. Polar Bioscience **12** : 100–113.

Lafaysse M, Morin S, Coléou C, Vernay M, Serça D, Besson F, Willemet J-M, Giraud G, Durand Y. 2013. Towards a new chain of models for avalanche hazard forecasting in French mountain ranges, including low altitude mountains. presented at the International Snow Science Workshop. Grenoble - Chamonix Mont Blanc. 162–166 pp.

Larcher W, Siegwolf R. 1985. Development of acute frost drought in Rhododendron ferrugineum at the alpine timberline. Oecologia **67** : 298–300. DOI: 10.1007/BF00384304

Lenoir J, Gegout JC, Marquet PA, de Ruffray P, Brisse H. 2008. A Significant Upward Shift in Plant Species Optimum Elevation During the 20th Century. Science **320** : 1768–1771. DOI: 10.1126/science.1156831

Liang E, Eckstein D. 2009. Dendrochronological potential of the alpine shrub Rhododendron nivale on the south-eastern Tibetan Plateau. Annals of Botany **104** : 665–670. DOI: 10.1093/aob/mcp158

Liang E, Lu X, Ren P, Li X, Zhu L, Eckstein D. 2012. Annual increments of juniper dwarf shrubs above the tree line on the central Tibetan Plateau: a useful climatic proxy. Annals of Botany **109** : 721–728. DOI: 10.1093/aob/mcr315

Liston GE, Mcfadden JP, Sturm M, Pielke RA. 2002. Modelled changes in arctic tundra snow, energy and moisture fluxes due to increased shrubs. Global Change Biology **8** : 17–32. DOI: 10.1046/j.1354-1013.2001.00416.x

López-Moreno JI. 2005. Recent Variations of Snowpack Depth in the Central Spanish Pyrenees. Arctic, Antarctic, and Alpine Research **37** : 253–260. DOI: 10.1657/1523-0430(2005)037[0253:RVOSDI]2.0.CO;2

Lu X, Camarero JJ, Wang Y, Liang E, Eckstein D. 2015. Up to 400-year-old *Rhododendron* shrubs on the southeastern Tibetan Plateau: prospects for shrub-based dendrochronology. Boreas **44** : 760–768. DOI: 10.1111/bor.12122

Madrigal-González J, Andivia E, Zavala MA, Stoffel M, Calatayud J, Sánchez-Salguero R, Ballesteros-Cánovas J. 2018. Disentangling the relative role of climate change on tree growth in an extreme Mediterranean environment. Science of The Total Environment **642** : 619–628. DOI: 10.1016/j.scitotenv.2018.06.064

Madrigal-González J, Ballesteros-Cánovas JA, Herrero A, Ruiz-Benito P, Stoffel M, Lucas-Borja ME, Andivia E, Sancho-García C, Zavala MA. 2017. Forest productivity in southwestern Europe is controlled by coupled North Atlantic and Atlantic Multidecadal Oscillations. Nature Communications **8** DOI: 10.1038/s41467-017-02319-0 [online] Available from: http://www.nature.com/articles/s41467-017-02319-0 (Accessed 16 August 2019)

Malfasi F, Cannone N. 2020. Climate Warming Persistence Triggered Tree Ingression After Shrub Encroachment in a High Alpine Tundra. Ecosystems DOI: 10.1007/s10021-020-00495-7 [online] Available from: http://link.springer.com/10.1007/s10021-020-00495-7 (Accessed 24 February 2020)

Marty C, Schlögl S, Bavay M, Lehning M. 2017. How much can we save? Impact of different emission scenarios on future snow cover in the Alps. The Cryosphere **11** : 517–529. DOI: 10.5194/tc-11-517-2017

Mitchell RJ. 1992. Testing Evolutionary and Ecological Hypotheses Using Path Analysis and Structural Equation Modelling. Functional Ecology **6** : 123. DOI: 10.2307/2389745

Molau U, Nordenhall U, Eriksen B. 2005. Onset of flowering and climate variability in an alpine landscape: a 10-year study from Swedish Lapland. American Journal of Botany **92** : 422–431. DOI: 10.3732/ajb.92.3.422

Mote PW, Hamlet AF, Clark MP, Lettenmaier DP. 2005. DECLINING MOUNTAIN SNOWPACK IN WESTERN NORTH AMERICA*. Bulletin of the American Meteorological Society **86** : 39–50. DOI: 10.1175/BAMS-86-1-39

Myers-Smith IH et al. 2011. Shrub expansion in tundra ecosystems: dynamics, impacts and research priorities. Environmental Research Letters **6** : 045509. DOI: 10.1088/1748-9326/6/4/045509

Myers-Smith IH et al. 2015a. Climate sensitivity of shrub growth across the tundra biome. Nature Climate Change **5** : 887–891. DOI: 10.1038/nclimate2697

Myers-Smith IH et al. 2015b. Methods for measuring arctic and alpine shrub growth: A review. Earth-Science Reviews **140** : 1–13. DOI: 10.1016/j.earscirev.2014.10.004

Myers-Smith IH et al. 2019. Eighteen years of ecological monitoring reveals multiple lines of evidence for tundra vegetation change. Ecological Monographs **89** : e01351. DOI: 10.1002/ecm.1351

Myers-Smith IH et al. 2020. Complexity revealed in the greening of the Arctic. Nature Climate Change **10** : 106–117. DOI: 10.1038/s41558-019-0688-1

Neuner G, Ambach D, Aichner K. 1999. Impact of snow cover on photoinhibition and winter desiccation in evergreen Rhododendron ferrugineum leaves during subalpine winter. Tree Physiology **19** : 725–732. DOI: 10.1093/treephys/19.11.725

Niittynen P, Heikkinen RK, Luoto M. 2018. Snow cover is a neglected driver of Arctic biodiversity loss. Nature Climate Change **8** : 997–1001. DOI: 10.1038/s41558-018-0311-x

Ozenda PG. 1985. La végétation de la chaîne alpine: dans l'espace montagnard européen . Masson: Paris u.a

Parmesan C, Yohe G. 2003. A globally coherent fingerprint of climate change impacts across natural systems. Nature **421** : 37–42. DOI: 10.1038/nature01286

Pautou G, Cadel G, Girel J. 1992. Le bassin de Bourd d'Oisans, carrefour phytogéographique des Alpes. Revue d'Ecologie Alpine : 23–43.

Pearson RG, Phillips SJ, Loranty MM, Beck PSA, Damoulas T, Knight SJ, Goetz SJ. 2013. Shifts in Arctic vegetation and associated feedbacks under climate change. Nature Climate Change **3** : 673–677. DOI: 10.1038/nclimate1858

Pellizzari E, Camarero JJ, Gazol A, Sangüesa-Barreda G, Carrer M. 2016. Wood anatomy and carbon-isotope discrimination support long-term hydraulic deterioration as a major cause of drought-induced dieback. Global Change Biology **22** : 2125–2137. DOI: 10.1111/gcb.13227

Pellizzari E, Pividori M, Carrer M. 2014. Winter precipitation effect in a mid-latitude temperature-limited environment: the case of common juniper at high elevation in the Alps. Environmental Research Letters **9** : 104021. DOI: 10.1088/1748-9326/9/10/104021

Pérez-de-Lis G, García-González I, Rozas V, Olano JM. 2016. Feedbacks between earlywood anatomy and non-structural carbohydrates affect spring phenology and wood production in ring-porous oaks. Biogeosciences **13** : 5499–5510. DOI: 10.5194/bg-13-5499-2016

Phoenix GK, Bjerke JW. 2016. Arctic browning: extreme events and trends reversing arctic greening. Global Change Biology **22** : 2960–2962. DOI: 10.1111/gcb.13261

Pornon A, Doche B. 1995. Influence des populations de Rhododendron ferrugineum L. sur la végétation subalpine (Alpes du Nord-France). Feddes Repertorium **106** : 179–191. DOI: 10.1002/fedr.19951060312

Pornon A, Doche B. 1996. Age structure and dynamics of Rhododendron ferrugineum L. populations in the northwestern French Alps. Journal of Vegetation Science **7** : 265–272.

Pornon A, Escaravage N, Till-Bottraud I. 1997. Variation of reproductive traits in Rhododendron ferrugineum L. (Ericaceae) populations along a successional gradient. Plant Ecology : 1–11.

R Core Team. 2016. R: A Language and Environment for Statistical Computing. R Foundation for Statistical Computing . R Foundation for Statistical Computing: Vienna, Austria [online] Available from: http://www.R-project.org/

Reid PC et al. 2016. Global impacts of the 1980s regime shift. Global Change Biology **22** : 682–703. DOI: 10.1111/gcb.13106

Rixen C, Dawes MA, Wipf S, Hagedorn F. 2012. Evidence of enhanced freezing damage in treeline plants during six years of CO_2 enrichment and soil warming. Oikos **121** : 1532–1543. DOI: 10.1111/j.1600-0706.2011.20031.x

Rixen C, Schwoerer C, Wipf S. 2010. Winter climate change at different temporal scales in *Vaccinium myrtillus* , an Arctic and alpine dwarf shrub. Polar Research **29** : 85–94. DOI: 10.1111/j.1751-8369.2010.00155.x

Ropars P, Lévesque E, Boudreau S. 2015. How do climate and topography influence the greening of the forest tundra ecotone in northern Québec? A dendrochronological analysis of *Betula glandulosa*. Journal of Ecology : n/a-n/a. DOI: 10.1111/1365-2745.12394

Rosseel Y. 2012. **lavaan** : An *R* Package for Structural Equation Modeling. Journal of Statistical Software **48** DOI: 10.18637/jss.v048.i02 [online] Available from: http://www.jstatsoft.org/v48/i02/ (Accessed 26 July 2019)

Schmidt NM, Baittinger C, Kollmann J, Forchhammer MC. 2010. Consistent Dendrochronological Response of the Dioecious Salix arctica to Variation in Local Snow Precipitation across Gender and Vegetation Types. Arctic, Antarctic, and Alpine Research **42** : 471–475. DOI: 10.1657/1938-4246-42.4.471

Schweingruber FH, Börner A, Schulze E-D. 2011. Atlas of Stem Anatomy in Herbs, Shrubs and Trees . Springer Berlin Heidelberg: Berlin, Heidelberg

Steger C, Kotlarski S, Jonas T, Schär C. 2013. Alpine snow cover in a changing climate: a regional climate model perspective. Climate Dynamics **41** : 735–754. DOI: 10.1007/s00382-012-1545-3

Steinbauer MJ et al. 2018. Accelerated increase in plant species richness on mountain summits is linked to warming. Nature **556** : 231–234. DOI: 10.1038/s41586-018-0005-6

Stinson KA. 2005. Effects of Snowmelt Timing and Neighbor Density on the Altitudinal Distribution of Potentilla diversifolia in Western Colorado, U.S.A. Arctic, Antarctic, and Alpine Research **37** : 379–386. DOI: 10.1657/1523-0430(2005)037[0379:EOSTAN]2.0.CO;2

Stocker TF, Qin GK, Plattner M. 2013. Climate Change 2013: The Physical Science Basis. Contribution of Working Group I to the Fifth Assessment Report of the Intergovernmental Panel on Climate Change . Cambridge University Press

Sturm M, Holmgren J, McFadden JP, Liston GE, Chapin FS, Racine CH. 2001. Snow–Shrub Interactions in Arctic Tundra: A Hypothesis with Climatic Implications. Journal of Climate **14** : 336–344. DOI: 10.1175/1520-0442(2001)014<0336:SSIIAT>2.0.CO;2

Tape K, Sturm M, Racine C. 2006. The evidence for shrub expansion in Northern Alaska and the Pan-Arctic. Global Change Biology **12** : 686–702. DOI: 10.1111/j.1365-2486.2006.01128.x

Treharne R, Bjerke JW, Tømmervik H, Stendardi L, Phoenix GK. 2019. Arctic browning: Impacts of extreme climatic events on heathland ecosystem CO_2 fluxes. Global Change Biology **25** : 489–503. DOI: 10.1111/gcb.14500

Vaganov EA, Hughes MK, Kirdyanov AV, Schweingruber FH, Silkin PP. 1999. Influence of snowfall and melt timing on tree growth in subarctic Eurasia. Nature **400** : 149–151.

Verfaillie D, Lafaysse M, Déqué M, Eckert N, Lejeune Y, Morin S. 2018. Multi-component ensembles of future meteorological and natural snow conditions for 1500 m altitude in the Chartreuse mountain range, Northern French Alps. The Cryosphere **12** : 1249–1271. DOI: 10.5194/tc-12-1249-2018

Vionnet V, Brun E, Morin S, Boone A, Faroux S, Le Moigne P, Martin E, Willemet J-M. 2012. The detailed snowpack scheme Crocus and its implementation in SURFEX v7.2. Geoscientific Model Development **5** : 773–791. DOI: 10.5194/gmd-5-773-2012

Walther G-R, Post E, Convey P, Menzel A, Parmesan C, Beebee TJC, Fromentin J-M, Hoegh-Guldberg O, Bairlein F. 2002. Ecological responses to recent climate change. Nature **416** : 389–395. DOI: 10.1038/416389a

Weijers S, Beckers N, Löffler J. 2018a. Recent spring warming limits near-treeline deciduous and evergreen alpine dwarf shrub growth. Ecosphere **9** : e02328. DOI: 10.1002/ecs2.2328

Weijers S, Broekman R, Rozema J. 2010. Dendrochronology in the High Arctic: July air temperatures reconstructed from annual shoot length growth of the circumarctic dwarf shrub Cassiope tetragona. Quaternary Science Reviews **29** : 3831–3842. DOI: 10.1016/j.quascirev.2010.09.003

Weijers S, Pape R, Löffler J, Myers-Smith IH. 2018b. Contrasting shrub species respond to early summer temperatures leading to correspondence of shrub growth patterns. Environmental Research Letters **13** : 034005. DOI: 10.1088/1748-9326/aaa5b8

Wheeler JA, Cortés AJ, Sedlacek J, Karrenberg S, van Kleunen M, Wipf S, Hoch G, Bossdorf O, Rixen C. 2016. The snow and the willows: earlier spring snowmelt reduces performance in the low-lying alpine shrub *Salix herbacea*. Cornelissen H (ed). Journal of Ecology **104** : 1041–1050. DOI: 10.1111/1365-2745.12579

Wilmking M. 2005. Increased temperature sensitivity and divergent growth trends in circumpolar boreal forests. Geophysical Research Letters **32** DOI: 10.1029/2005GL023331 [online] Available from: http://doi.wiley.com/10.1029/2005GL023331 (Accessed 29 May 2018)

Wilmking M et al. 2020. Global assessment of relationships between climate and tree growth. Global Change Biology : gcb.15057. DOI: 10.1111/gcb.15057

Wipf S. 2010. Phenology, growth, and fecundity of eight subarctic tundra species in response to snowmelt manipulations. Plant Ecology **207** : 53–66. DOI: 10.1007/s11258-009-9653-9

Wipf S, Rixen C. 2010. A review of snow manipulation experiments in Arctic and alpine tundra ecosystems. Polar Research **29** : 95–109. DOI: 10.1111/j.1751-8369.2010.00153.x

Wipf S, Rixen C, Mulder CPH. 2006. Advanced snowmelt causes shift towards positive neighbour interactions in a subarctic tundra community. Global Change Biology **12** : 1496–1506. DOI: 10.1111/j.1365-2486.2006.01185.x

Wipf S, Stoeckli V, Bebi P. 2009. Winter climate change in alpine tundra: plant responses to changes in snow depth and snowmelt timing. Climatic Change **94** : 105–121. DOI: 10.1007/s10584-009-9546-x

Young AB, Watts DA, Taylor AH, Post E. 2016. Species and site differences influence climate-shrub growth responses in West Greenland. Dendrochronologia **37** : 69–78. DOI: 10.1016/j.dendro.2015.12.007

Zalatan R, Gajewski K. 2006. Dendrochronological Potential of Salix alaxensis from the Kuujjua River Area, Western Canadian Arctic. Tree-Ring Research **62** : 75–82. DOI: 10.3959/1536-1098-62.2.75

Zang C, Biondi F. 2015. treeclim: an R package for the numerical calibration of proxy-climate relationships. Ecography **38** : 431–436. DOI: 10.1111/ecog.01335

Zuur AF, Ieno EN, Elphick CS. 2010. A protocol for data exploration to avoid common statistical problems: Data exploration. Methods in Ecology and Evolution **1** : 3–14. DOI: 10.1111/j.2041-210X.2009.00001.x